A New Method for Crosstalk Prediction Between Triple-twisted Strand (Uniform and Non-uniform) and Signal Wire based on CDBAS-BPNN Algorithm

Yanxing Ji [1], Wei Yan [1*], Yang Zhao [1], Chao Huang [1], Shiji Li [1], Jianming Zhou [1], and Xingfa Liu [2]

[1] School of Electrical & Automation Engineering
Nanjing Normal University, Nanjing 210046, China
397832514@qq.com, *61197@njnu.edu.cn, zhaoyang2@njnu.edu.cn, 1547796467@qq.com,
lishijin@njnu.edu.cn, zhoujianmingz@163.com, liuxingfa@epri.sgcc.com.cn

[2] China State Key Laboratory of Power Grid Environmental Protection
Wuhan Branch of China Electric Power Research Institute, Wuhan 430000, China

Abstract ─ This paper proposes a novel crosstalk prediction method between the triple-twisted strand (uniform and non-uniform) and the signal wire, that is, using back-propagation neural network optimized by the beetle antennae search algorithm based on chaotic disturbance mechanism (CDBAS-BPNN) to extract the per unit length (p.u.l) parameter matrix, and combined with the chain parameter method to obtain crosstalk. Firstly, the geometric model and cross-sectional model between the uniform triple-twisted strand and the signal wire are established, and the corresponding model between the non-uniform triple-twisted strand and the signal wire is obtained by the Monte Carlo (MC) method. Then, the beetle antennae search algorithm based on chaotic disturbance mechanism (CDBAS) and back-propagation neural network (BPNN) are combined to construct a new extraction network of the p.u.l parameter matrix, and the chain parameter method is combined to predict crosstalk. Finally, in the verification and analysis part of the numerical experiments, comparing the crosstalk results of CDBAS-BPNN, BAS-BPNN and Transmission Line Matrix (TLM) algorithms, it is verified that the proposed method has better accuracy for the prediction of the model.

Index Terms ─ Beetle Antenna Search (BAS), Back-Propagation Neural Network (BPNN), chaotic disturbance mechanism, crosstalk, triple-twisted strand.

I. INTRODUCTION

Multi-core stranded wire has the characteristics of low loss, low cost and small coupling [1]. Thus, they are widely used in modern electronic equipment and systems (such as communication systems, aircraft and ships). Although it has good performance in reducing radiated interference, further research is needed to analyze the crosstalk between lines [2-4]. At the same time, with the complexity and miniaturization of equipment, unnecessary electromagnetic interaction or crosstalk between wires will be greatly enhanced, thereby reducing the performance of the equipment.

For the study of cable crosstalk, the traditional method is to directly solve its transmission lines equation through the transmission lines model to obtain crosstalk [5]. However, the cross-sectional position in the twisted-wire pair (TWP) is random and unknown. The randomness of the cross-sectional position brings different p.u.l parameter matrices, so it is difficult to predict its crosstalk directly by traditional methods [6, 7].

Recently, many researchers have studied the prediction of TWP crosstalk. They focused their research on TWP, but relatively little research has been done on the crosstalk of triple-twisted strand. In [8], Taylor extended the results of uniform parallel lines to TWP, which is suitable for non-uniform transmission lines model. However, this method relies on the assumption of torsion and the accuracy is not high. In [9], Cannas proposed to treat non-uniform stranded wires as a cascade of uniform cross-sections and used BPNN to make predictions. In [10], the random displacement spline interpolation (RDSI) was proposed by Dai to generate a set of non-uniform wire harnesses to provide training samples, and then used the trained BPNN to predict the crosstalk, but ordinary BPNN may have high error, and its prediction range is narrow.

According to the theory of cascading transmission lines proposed by Paul and McKnight, cascaded multi-section transmission lines are used to replace the overall wiring harness [11-13]. Therefore, as long as the p.u.l

parameter matrices at different positions are obtained, the crosstalk of the cable can be obtained by the chain parameter method.

In this paper, the coupling model between the uniform triple-twisted strand and the signal wire is established through the production principle of triple-twisted strand. Based on this, the Monte Carlo (MC) method was used to obtain the coupling model between the non-uniform triple-twisted strand and the signal wire, and the randomness of the non-uniform triple-twisted strand was simulated. In our previous research [14-16], neural networks have been shown to express the relationship between the transmission lines position and the p.u.l parameter matrix. The BPNN algorithm relies heavily on its initial weight and threshold parameters, but its initial weight and threshold is randomly generated, which results in a large difference in the results of each simulation and poor robustness [17-19]. This paper combines the CDBAS algorithm and the BPNN algorithm to obtain a new p.u.l parameter matrix prediction network [20, 21]. Compared with the traditional BPNN algorithm, the convergence speed is faster and the solution accuracy is higher. Then, using the chain parameter model, the near-end crosstalk (NEXT) and far-end crosstalk (FEXT) between the triple-twisted strand and the signal wire are given. The results of numerical experiments verify the effectiveness of the method.

The rest of the paper is organized as follows: In Section II, the model of the triple-twisted strand (uniform and non-uniform) and the signal wire is established. In Section III, the p.u.l parameter matrix at any position of the transmission line is obtained through CDBAS-BPNN, and the voltage and current at both ends of the line are derived. In Section IV, the numerical experiments are used to verify the proposed method, which proves the accuracy of this method. On this basis, the crosstalk results are analyzed, and the terminal voltage characteristics under line-to-line coupling are obtained. Finally, the results are given in Section V.

II. THE MODEL OF TRIPLE-TWISTED STRAND AND SINGLE WIRE

In this paper, based on the production principle of triple-twisted strand, a coupling model of the uniform triple twisted-strand and the signal wire is established, as shown in Fig. 1. The diameter of the core is D, the height from the ground is h, and the distance of the center of the triple-twisted strand from the separate single wire is d. According to the idea of the cascading method, the triple-twisted strand is divided into uniform small pieces along the axial direction. And the following characteristics are assumed: Each transmission line can be considered as a parallel transmission line, there is only one mode of transverse electric and magnetic wave propagation on the

transmission line; the geometric shape of the cross-section can be considered as a circular outline; the structure and material of each cable are the same.

Figure 2 shows the coupling model between the non-uniform triple-twisted strand and the signal wire. Except for the uneven twisting of the stranded wire, the other parameters are the same as those in Fig. 1. This paper uses the MC method to randomly simulate a non-uniform model. The coordinate positions of the triple-twisted strand (uniform and non-uniform) and the signal wire can be expressed as formula (1):

$$\begin{cases} m_r(x,y,z) = (\frac{\sqrt{3}}{3}D\cos\theta_z, h+\frac{\sqrt{3}}{3}D\sin\theta_z, z) \\ m_g(x,y,z) = (\frac{\sqrt{3}}{3}D\cos(\theta_z+120°), h+\frac{\sqrt{3}}{3}D\sin(\theta_z+120°), z) \\ m_b(x,y,z) = (\frac{\sqrt{3}}{3}D\cos(\theta_z-120°), h+\frac{\sqrt{3}}{3}D\sin(\theta_z-120°), z) \\ m_s(x,y,z) = (d,0,z) \end{cases},(1)$$

where m_r, m_g and m_b represent the position coordinates of each point on the triple-twisted strand. m_s indicates the position coordinates of each point on the signal wire. θ_z represents the rotation angle at the axial position z corresponding to the initial position $z=0$.

Figure 3 is the change of the cross-section of the wire within one revolution of the uniform triple-twisted strand. Different sections correspond to different p.u.l parameter matrices.
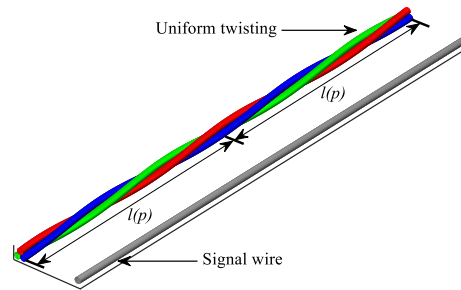
Fig. 1. Geometric model of uniform stranded wire and signal wire.
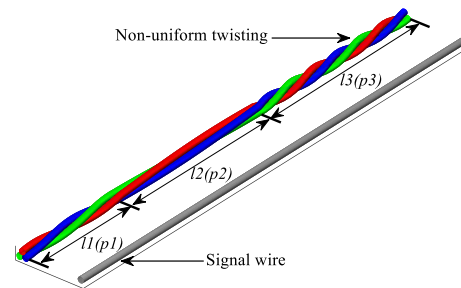
Fig. 2. Geometric model of non-uniform stranded wire and signal wire.
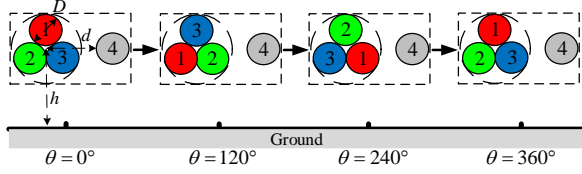
Fig. 3. Changes in the cross-section of the wire harness during a uniform rotation.

In the model of single wire and uniform triple-twisted strand, the rotation angle corresponding to different positions is:

$$\theta_z = \frac{360°z}{p}, \qquad (2)$$

where p is the axial length of the triple-twisted strand rotating evenly, that is, the pitch of the transmission line.

In the non-uniform model, only the twisting degree of the triple-twisted strand is non-uniform. Therefore, all its cross-sectional models can be obtained in the uniform model, but the twisting angles corresponding to different positions are different. The MC method can simulate the model of non-uniform triple-twisted strand and the angle of rotation corresponding to the cross-section.

III. ACQUISITION OF PARAMETER MATRIX AND PREDICTION OF CROSSTALK

A. Unit length parameter matrix

In order to facilitate the study, only the uniformly divided model is considered first, and each segment is regarded as a parallel transmission line. The micro-element conduction model of a multi-conductor transmission line per unit length is shown in Fig. 4. r_{ij}, l_{ij}, c_{ij}, and g_{ij}, respectively represent the elements in the resistance **R**, inductance **L**, capacitance **C**, and conductance **G** parameter matrices, where $i, j = 1, 2, 3 \cdots n$.
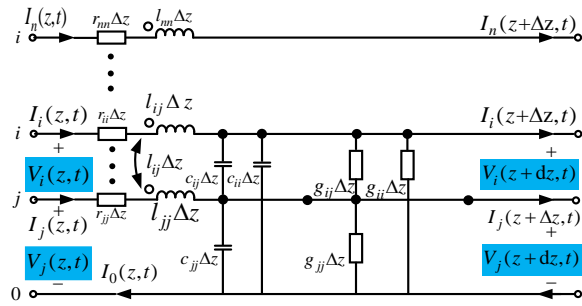
Fig. 4. Unit length equivalent circuit model of multi-conductor transmission line.

The voltage and current of the transmission line satisfy the following equation [10]:

$$\frac{\partial \mathbf{V}(z,t)}{\partial z} + \mathbf{R}(z)\mathbf{I}(z,t) + \mathbf{L}(z)\frac{\partial \mathbf{I}(z,t)}{\partial t} = 0$$
$$\frac{\partial \mathbf{I}(z,t)}{\partial z} + \mathbf{G}(z)\mathbf{V}(z,t) + \mathbf{C}(z)\frac{\partial \mathbf{V}(z,t)}{\partial t} = 0 \qquad (3)$$

where $\mathbf{V}(z,t)$ and $\mathbf{I}(z,t)$ are the voltage and current vectors at position z and time t. $\mathbf{R}(z)$, $\mathbf{L}(z)$, $\mathbf{C}(z)$ and $\mathbf{G}(z)$ represent the unit length parameter matrix at position z, which are all symmetric matrices of order $n \times n$.

In the uniform model, since the rotation of the triple-twisted strand is uniform, the parameters in the parameter matrix **X** of 0°~120°, 120°~240°, 240°~360° are all the same, but the positions are different, as long as the corresponding transformation is performed:

$$\mathbf{X}(z(\theta')) = \begin{cases} \mathbf{T}\mathbf{X}(z(\theta))\mathbf{T}^T & ,\theta' \in [120°, 240°) \\ \mathbf{T}^2\mathbf{X}(z(\theta))(\mathbf{T}^T)^2 & ,\theta' \in [240°, 360°) \end{cases} , \quad (4)$$

where **T** is the transformation matrix, which is:

$$\mathbf{T} = \begin{bmatrix} 0 & 0 & 1 & 0 \\ 1 & 0 & 0 & 0 \\ 0 & 1 & 0 & 0 \\ 0 & 0 & 0 & 1 \end{bmatrix}. \qquad (5)$$

In the non-uniform model, since the cross-section can be obtained from the uniform model, the parameter matrix **X** can be obtained from the uniform model.

B. Predicting p.u.l parameter by CDBSA-BPNN algorithm

Due to the geometric characteristics of the stranded wire, the **RLCG** parameter matrix at different positions is different. Formula (6) can be obtained from formula (4):

$$\mathbf{X}(z) = f(\theta). \qquad (6)$$

It can be seen from formula (6) that different rotation angles correspond to different parameter matrices. There is a nonlinear mapping relationship between the rotation angle and the parameter matrix. Therefore, this paper introduces a BPNN algorithm with strong nonlinear mapping ability. Because there are many elements in the parameter matrix of the triple-twisted strand, as the output of the BPNN, the output of the network may be trapped in the local minimum. Therefore, the CDBAS algorithm is employed to optimize the weight of the BPNN. BAS algorithm is sensitive to the dimensionality of the optimization target. The dimensionality of the weight w composed of w_i and w_{ij} is large in the model of this paper. Thus, the CDBAS algorithm is used for optimization. The topology of CDBAS-BPNN is shown in Fig. 5.
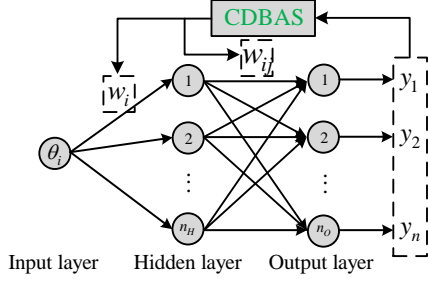
Fig. 5. Topological structure of CDBAS-BPNN.

The input of the network is the rotation angle θ_i ($0 \leq \theta_i \leq 120°$) of the cross-section i. The output is the **RLCG** parameter matrix value of cross-section i. Since the parameter matrix is a symmetric matrix, its upper triangle is taken as a row of vectors as the output, the number of vector dimension is:

$$1+2+3+\cdots+n = \sum n. \tag{7}$$

The number of hidden layers n_h is an empirical value determined by the number of output layers n_o, which can be as follows:

$$n_h = 0.5(n_o + 1) + a, \quad a = 1, 2, \cdots 10. \tag{8}$$

The input layer to the hidden layer uses the sigmoid function $h(x)$, and the hidden layer to the output layer uses the linear function $o(x)$. The input can get a nonlinear output through forward propagation, and then the CDBAS algorithm is used to back-propagate the error $f(x)$ to obtain the global minimum:

$$\begin{cases} h(x) = \dfrac{1}{1 + e^{-x}} \\ o(x) = x \end{cases}. \tag{9}$$

The weights w_i and w_{ij} are determined by the CDBAS algorithm. The specific steps are as follows:

Step 1: Determine optimization goals and build search model.

For N sets of data, the mean square deviation of the network output and the actual value is:

$$f(x) = \frac{1}{2N} \sum_{i=1}^{N} \sum_{j=1}^{n_2} (y_j - y_j')^2, \tag{10}$$

where y_i' is the actual value of the parameter matrix, and $f(x)$ is the optimized objective function.

List the ownership value as a single row vector x, which represents the position of the beetle in the high-dimensional data space. At a certain time t the position of the beetle is:

$$x^t = \text{rand}(k, 1), \tag{11}$$

where k is the dimension of the weight vector, and rand is a k-dimensional column vector that generates a uniform distribution.

The search directions of beetle are:

$$\vec{b} = \frac{\text{rand}(k, 1)}{\|\text{rand}(k, 1)\|_2}. \tag{12}$$

By searching to the left or right, the activity of the antennae of the beetle's whiskers can be simulated:

$$x_r^t = x^t + d^t \vec{b}, \quad x_l^t = x^t - d^t \vec{b}, \tag{13}$$

where x_r^t is the position of the search area on the right whisker side, x_l^t is the position of the search area on the left whisker side, d^t is the antenna length of the beetle at time t. It should be long enough to cover the appropriate search range so that it can jump out from the local minimum point from the beginning, and then the sensor length gradually decreases with the passage of time t.

Step 2: Generate an iterative model of the position of the beetle:

$$x^{t+1} = x^t + \delta^{t+1} \vec{b} \, \text{sign}\left(f(x_r^t) - f(x_l^t)\right), \tag{14}$$

where δ is the step size of the search, which illustrates the convergence rate of the decreasing function of t. The initialization of δ should be equivalent to the search area. $\text{sign}(\cdot)$ represents the symbolic function.

The update rules for search parameters d and δ are:

$$\begin{cases} d^t = 0.95 d^{t-1} + 0.01 \\ \delta^t = 0.95 \delta^{t-1} \end{cases}. \tag{15}$$

Step 3: Generate chaotic sequence.

In the BAS algorithm, since the beetle is a single individual search, its global search effect is poor, and it cannot find the ideal result in a large range. Tent mapping is added to form CDBAS, so that it can search for the best fitness value in a large range.

The formula for Tent mapping is [22]:

$$X_n = \begin{cases} 2x_n & 0 \leq x_n \leq 1/2 \\ 2(1 - x_n) & 1/2 \leq x_n \leq 1 \end{cases}, \tag{16}$$

where X_n is the n-th dimension variable of the chaotic sequence x^{t+1}, $n = 1, 2, \cdots k$. x_n is a random number obeying uniform distribution, $x_n \in [0, 1]$.

Step 4: Perform chaos disturbance in the position of the beetle whiskers.

Map the chaotic variable back to the position x about the beetle:

$$\text{new}X_n = \min_n + (\max_n - \min_n) X_n, \tag{17}$$

where max_n and min_n are respectively the maximum and minimum values of the n-th dimension variable $newX_n$.

Chaotic disturbance to the position of the beetle:

$$\text{new}x^{t+1} = x^{t+1} + step \times (\text{new}X_n - x^{t+1})/2, \tag{18}$$

where x^{t+1} is the position of the beetle that needs chaos disturbance, $newX_n$ is the amount of chaos disturbance generated, $newx^{t+1}$ is the new position of the beetle after chaos disturbance, and *step* is the step length of the beetle.

Step 5: Update the optimal position and optimal objective function of beetle.

$$\begin{cases} x_{best} = x^{t+1} \\ f_{best} = f(x^t) \end{cases}. \tag{19}$$

The resulting x_{best} is the weight of the BPNN, and f_{best} is the global optimal error obtained by iteration. The specific process is shown in Fig. 6.
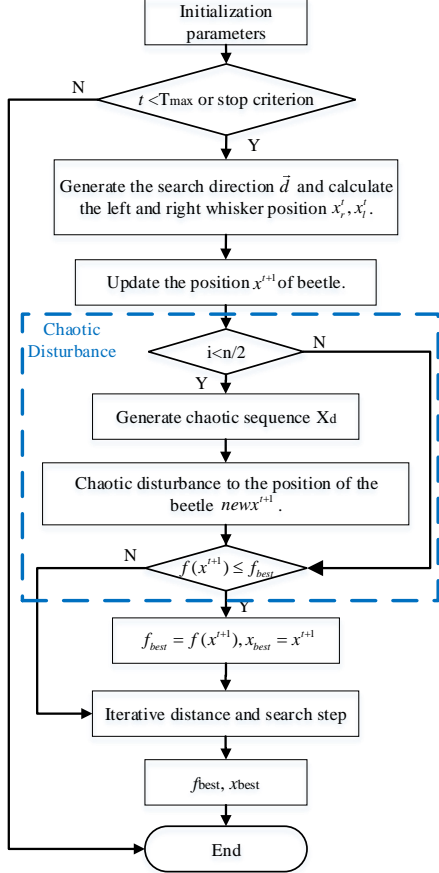
Fig. 6. CDBAS optimization neural network process.

C. Calculation of crosstalk

Turn formula (3) into a frequency domain equation:

$$\begin{cases} \dfrac{d}{dz}\mathbf{V}(z) = -\mathbf{Z}(z)\mathbf{I}(z) \\ \dfrac{d}{dz}\mathbf{I}(z) = -\mathbf{Y}(z)\mathbf{U}(z) \end{cases}, \tag{20}$$

where,

$$\begin{cases} \mathbf{V}(z) = \left[V_1(z); V_2(z); V_3(z); V_4(z)\right] \\ \mathbf{I}(z) = \left[I_1(z); I_2(z); I_3(z); I_4(z)\right] \\ \mathbf{Z}(z) = \mathbf{R}(z) + jw\mathbf{L}(z) \\ \mathbf{Y}(z) = \mathbf{G}(z) + jw\mathbf{C}(z) \end{cases}. \tag{21}$$

Perform the following modulus transformation,

$$\begin{cases} \mathbf{V}(z) = \mathbf{T}_V(z)\mathbf{V}_m(z) \\ \mathbf{I}(z) = \mathbf{T}_I(z)\mathbf{I}_m(z) \end{cases}. \tag{22}$$

The original equation can be reduced to:

$$\begin{cases} \dfrac{d^2}{dz^2}\mathbf{V}_m(z) = \mathbf{T}_V^{-1}(z)\mathbf{Z}(z)\mathbf{Y}(z)\mathbf{T}_V(z)\mathbf{V}_m(z) \\ \qquad\qquad = r^2\mathbf{V}_m(z) \\ \dfrac{d^2}{dz^2}\mathbf{I}_m(z) = \mathbf{T}_I^{-1}(z)\mathbf{Y}(z)\mathbf{Z}(z)\mathbf{T}_I(z)\mathbf{I}_m(z) \\ \qquad\qquad = r^2\mathbf{I}_m(z) \end{cases}, \tag{23}$$

where r^2 is a diagonal matrix of $n \times n$, and $T_V^+ = T_I^{-1}$, so the characteristic impedance $\mathbf{Z}_C$ and $\mathbf{Y}_C$ admittance matrix at different positions z are:

$$\begin{aligned} \mathbf{Z}_C(z) &= \mathbf{T}_V(z)r^{-1}(z)\mathbf{T}_V^{-1}(z)\mathbf{Z}(z) \\ \mathbf{Y}_C(z) &= \mathbf{T}_I(z)r^{-1}(z)\mathbf{T}_I^{-1}(z)\mathbf{Y}(z) \end{aligned}. \tag{24}$$
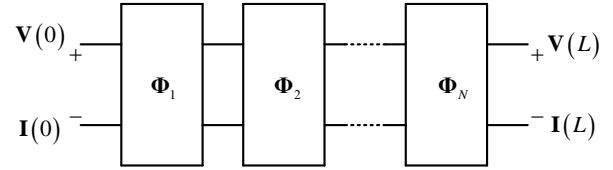
Fig. 7. Transmission line chain parameter model.

As shown in Fig. 7, get different chain parameter matrix:

$$\mathbf{\Phi}(z) = \begin{bmatrix} \phi_{11}(z) & \phi_{12}(z) \\ \phi_{21}(z) & \phi_{22}(z) \end{bmatrix}, \tag{25}$$

where $\phi_{11}(z)$, $\phi_{12}(z)$, $\phi_{21}(z)$, $\phi_{22}(z)$ are the chain parameter subarrays, they are:

$$\begin{cases} \phi_{11}(z) = \dfrac{1}{2}\mathbf{Y}^{-1}\mathbf{T}_I\left(e^{r\Delta z} + e^{-r\Delta z}\right)\mathbf{T}_I^{-1}\mathbf{Y} \\ \phi_{12}(z) = -\dfrac{1}{2}\mathbf{Y}^{-1}\mathbf{T}_I\left(e^{r\Delta z} - e^{-r\Delta z}\right)\mathbf{T}_I^{-1} \\ \phi_{21}(z) = -\dfrac{1}{2}\mathbf{T}_I\left(e^{r\Delta z} - e^{-r\Delta z}\right)r^{-1}\mathbf{T}_I^{-1}\mathbf{Y} \\ \phi_{22}(z) = \dfrac{1}{2}\mathbf{T}_I\left(e^{r\Delta z} + e^{-r\Delta z}\right)\mathbf{T}_I^{-1} \end{cases}. \tag{26}$$

Combining the CDBAS-BPNN algorithm to obtain the p.u.l at any position z, all the chain parameters $\mathbf{\Phi}(z)$ can be obtained by using formula (26).

The chain parameters of the transmission line are:

$$\mathbf{\Phi}(L) = \prod_{k=1}^{N} \mathbf{\Phi}_{N-k+1}\left(\Delta z_{N-k+1}\right). \tag{27}$$

$$\begin{bmatrix} \mathbf{V}(L) \\ \mathbf{I}(L) \end{bmatrix} = \mathbf{\Phi}(L)\begin{bmatrix} \mathbf{V}(0) \\ \mathbf{I}(0) \end{bmatrix}. \tag{28}$$

The terminal constraints are:

$$\begin{cases} \mathbf{V}(0) = \mathbf{V}_s - \mathbf{Z}_s \mathbf{I}(0) \\ \mathbf{V}(L) = \mathbf{V}_L + \mathbf{Z}_L \mathbf{I}(L) \end{cases}, \quad (29)$$

where $\mathbf{V}_S=[0;0;0;V_S]$ is the near-end termination voltage source, and $\mathbf{Z}_S$ is the near-end termination impedance. $\mathbf{V}_L=[0;0;0;0]$ is the far-end termination voltage source, and $\mathbf{Z}_L$ is the far-end termination impedance.

The resulting crosstalk is:

$$\begin{cases} \text{NEXT} = 20\log_{10}(\mathbf{V}(0)/V_s) \\ \text{FEXT} = 20\log_{10}(\mathbf{V}(L)/V_s) \end{cases}. \quad (30)$$

IV. VERIFICATION AND ANALYSIS

A. Verification of CDBAS-BPNN algorithm

In order to verify the effectiveness of the proposed method, this paper uses the model shown in Fig. 1. The distance between the triple-twisted strand and the signal wire is d=10mm, and the height of center wire from ground is h=8mm. The relevant parameters of the wire are shown in Table 1.

Table 1: Basic parameters

Name	Value
Wire diameter	0.8mm
Insulation layer thickness	0.6mm
Wire material	Copper
Insulation material	PVC
Wire length	1m
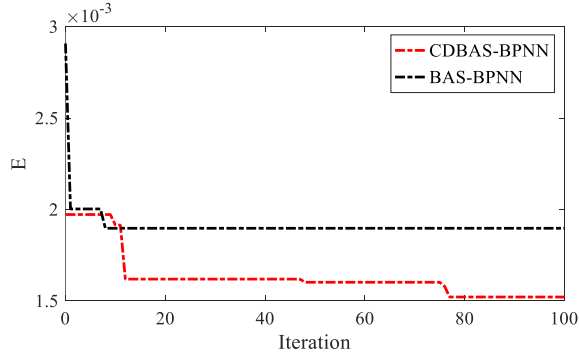
Fig. 8. CDBAS-BPNN iteration diagram.

The initial reference cross-sectional model is the cross section of 0° in Fig. 3. Using ANSYS simulation software to extract the parameter matrix, only need to consider the parameter matrix extraction of 0 ~ 120°, the parameter matrix of other angles can be obtained by formula (4). The **RLCG** matrix values are sampled every 4° between 0 ~ 120°, and there are 30 groups in total, which are used as training data for the CDBAS-BPNN algorithm. The number of hidden layers of BPNN is set to 8 and the number of CDBAS iterations is set to 100. The units of **R**, **L**, **C**, and **G** are Ω/m, nH/m, pF/m, and

mS/m, respectively. Figure 8 is the iterative process of the average error of the parameter matrix of the BAS-BPNN and CDBAS-BPNN algorithms. The average errors E of BAS-BPNN and CDBAS-BPNN are 1.85×10^{-3} and 1.51×10^{-3}, respectively. It can be seen that the prediction accuracy of CDBAS-BPNN is better.

B. Analysis of crosstalk results

TLM method is used in the CST Cable Studio software to perform numerical simulation on the model of the triple-twisted strand and the signal wire [22]. Its layout in CST is shown in Fig. 9. Both ends of the triple-twisted strand are connected with 50Ω resistors, and the signal wire is connected to a signal source with an amplitude of 1V and a frequency varying from 0.1MHz to 1GHz.

The crosstalk results of #1, #2, and #3 of the uniform model are shown in Figs. 10, 11, and 12, respectively. The red solid line is the result obtained by the proposed method in this paper. The black dotted line is the result of CST simulation and is used as a reference value. The blue dotted line is the method of BAS-BPNN mentioned in reference [15], which is called the old method. The transmission line is divided into 1200 segments, and the CPU time spent by each group is 75.41s (the old method calculates the payment time is very close), while the CST calculation takes 2.41 minutes, which can reduce a lot of calculation time.
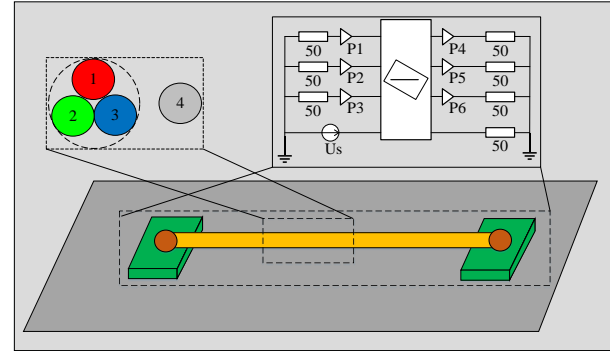
Fig. 9. CST simulation layout of the triple-twisted strand and the signal wire.
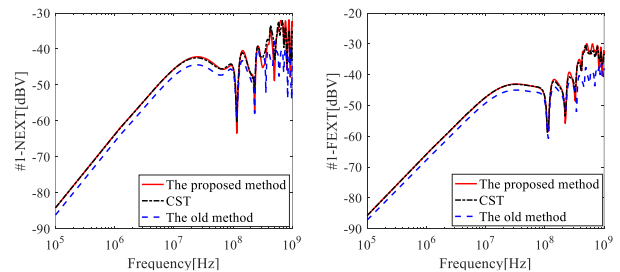
Fig. 10. Uniform #1 crosstalk.
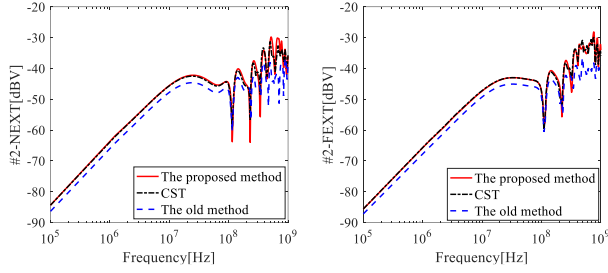
Fig. 11. Uniform #2 crosstalk.
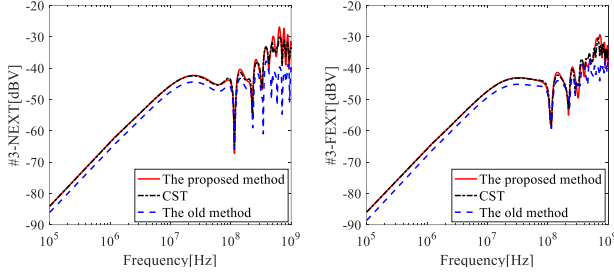
Fig. 12. Uniform #3 crosstalk.

In the low frequency range (0.1MHz $< f$ <100MHz), the results of the two methods are basically the same as the reference value, but the old method still has a certain difference, which is about 1 to 2dB worse than the reference value. In the middle and high frequency range (100MHz $< f <$ 1GHz), the old method starts to deviate from the reference value, especially in the high frequency range, the old method and the reference value began to have serious deviations, but the proposed method and the reference value can still maintain a good agreement.

It can be seen from Table 2 that the results are very consistent with the CST simulation results, the smallest average error is 0.06%, and the largest average error is 3.77%. However, the curve in the high frequency range (500MHz $< f$ <1GHz) is less consistent than the curve in the low frequency range (0.1MHz $< f$ <100MHz).

Table 2: Average error (%) of the uniform model

f/MHz		CDBAS-BPNN			BAS-BPNN		
	Wire	#1	#2	#3	#1	#2	#3
0.1~100	NEXT	0.07	0.59	0.10	3.92	4.69	4.69
	FEXT	0.06	0.08	0.28	4.02	4.60	4.28
100~500	NEXT	3.77	2.01	2.79	7.96	10.2	13.6
	FEXT	0.25	1.44	2.47	10.7	12.6	5.70
500~1000	NEXT	1.17	2.69	3.01	17.5	15.9	27.3
	FEXT	0.75	1.51	2.23	17.3	18.8	16.1

The crosstalk results of the non-uniform model are shown in Figs. 13, 14, 15 respectively. The red solid line is the result obtained by the method in this paper, and the CPU time spent by each group is 82.35s, and the CST calculation takes 3.36 minutes. The black dotted line is the result of CST simulation and is used as a reference value. The blue dotted line is the result of the old method. In the low frequency range (0.1MHz< f <100MHz), the results are basically similar to the uniform model. In the intermediate frequency range (100MHz< f <500MHz), the method proposed in this paper is more consistent with the reference value than the old method. In the high-frequency range (500MHz< f <1GHz), the near-end crosstalk obtained by the method in this paper is basically consistent, but the far-end crosstalk is slightly larger than the reference value.
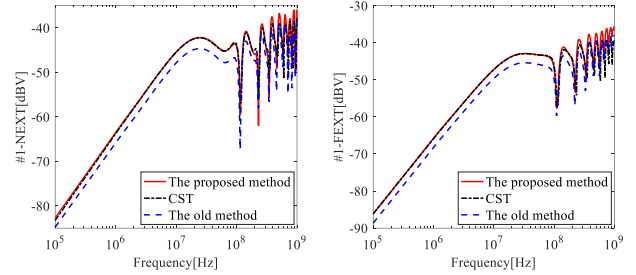
Fig. 13. Non-uniform # 1 crosstalk.
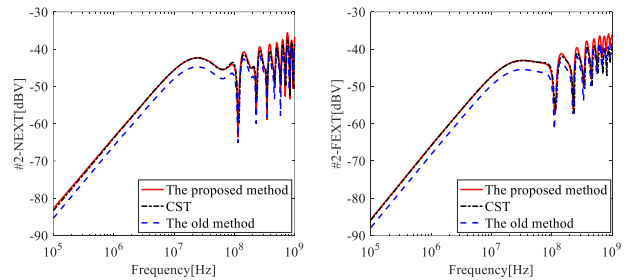
Fig. 14. Non-uniform # 2 crosstalk.
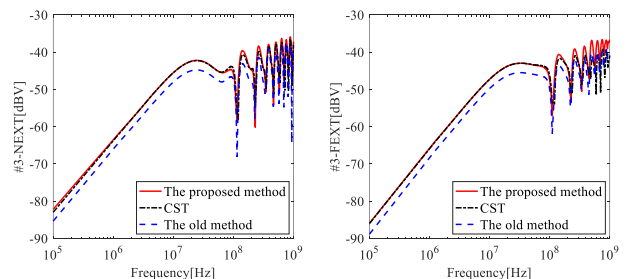
Fig. 15. Non-uniform # 3 crosstalk.

It can be seen from Table 3 that the smallest average error is 0.05% and the largest average error is 9.30%. However, in the high frequency range (500MHz $<f$ <1GHz), the NEXT curve of the triple-twisted strand is more consistent than the FEXT curve result. The possible reason is that the non-uniform model is repeatedly iterated, which makes the far-end crosstalk result fluctuate greatly.

Table 3: Average error (%) of the non-uniform model

f/MHz		CDBAS-BPNN			BAS-BPNN		
	Wire	#1	#2	#3	#1	#2	#3
0.1~100	NEXT	0.06	0.22	0.43	6.01	5.58	5.74
	FEXT	0.22	0.32	0.43	6.07	5.91	6.06
100~500	NEXT	0.77	1.27	0.89	4.94	3.78	4.29
	FEXT	2.90	2.57	3.04	2.80	2.53	3.31
500~1000	NEXT	4.07	2.67	2.23	3.61	2.66	4.34
	FEXT	8.14	8.22	9.30	2.36	1.99	2.44

Comparing the uniform model and the non-uniform model, it can be seen that the non-uniform results fluctuate more in the high-frequency range, while the uniform results fluctuate less in its range. This is the performance of the randomness of the non-uniform model in the results. The result corresponding to each frequency point in the non-uniform model will cause a large error in the actual measurement. It is difficult to make a small change in the corresponding frequency range like the result in a uniform model, and the measurement accuracy is high.

V. CONCLUSION

For the coupling model of triple-twisted strand and signal wire, this paper proposes a p.u.l parameter matrix prediction process based on CDBSA-BPNN algorithm. Combined with the chain parameter method of the transmission line, a new method to predict the crosstalk between the triple-twisted strand and the signal wire is proposed. Numerical experimental results show that the method has good applicability and effectiveness, especially in the low-frequency and intermediate-frequency bands with high consistency. The results also show that the use of a non-uniform model can reduce the difference in crosstalk between strands, but will cause the crosstalk results to suffer greater fluctuations in the high-frequency range. The estimation results of the crosstalk between the triple-twisted strand and the signal wire can provide important guiding significance and reference value for the electromagnetic compatibility design in engineering practice. However, this paper does not consider the effect of frequency on the p.u.l parameter matrix and the triple-twisted strand. Therefore, there is still a lot of research space after this paper.

ACKNOWLEDGMENT

REFERENCES

[1]   Y. Yan, L. Meng, X. Liu, T. Jiang, J. Chen, and G. Zhang, "An FDTD method for the transient terminal response of twisted-wire pairs illuminated by an external electromagnetic field," *IEEE Transactions on Electromagnetic Compatibility*, vol. 60, no. 2, pp. 435-443, Apr. 2018.

[2]   C. Paul and J. McKnight, "Prediction of crosstalk involving twisted pairs of wires-Part I: A transmission-line model for twisted-wire pairs," *IEEE Trans. Electromagn. Compat.*, vol. EMC-21, no. 2, pp. 92-105, May 1979.

[3]   R. Stolle, "Electromagnetic coupling of twisted pair cables," *IEEE J. Sel. Areas Comm.*, vol. 20, no. 5, pp. 883-892, June 2002.

[4]   F. Grassi and S. A. Pignari, "Immunity to conducted noise of data trans-mission along DC power lines involving twisted-wire pairs above ground," *IEEE Trans. Electromagn. Compat.*, vol. 55, no. 1, pp. 195-207, Feb. 2013.

[5]   C. R. Paul, *Analysis of Multiconductor Transmission Lines*. Hoboken, NJ, USA: Wiley, 1994.

[6]   Y. Yan, L. Meng, X. Liu, T. Jiang, J. Chen, and G. Zhang, "An FDTD method for the transient terminal response of twisted-wire pairs illuminated by an external electromagnetic field," *IEEE Trans. Electromagn. Compat.*, vol. 60, no. 2, pp. 435-443, Apr. 2018.

[7]   S. Chabane, P. Besnier, and M. Klingler, "A modified enhanced transmission line theory applied to multiconductor transmission lines," *IEEE Trans. Electromagn. Compat.*, vol. 59, no. 2, pp. 518-528, Apr. 2017.

[8]   C. D. Taylor and J. P. Castillo, "On the response of a terminated twisted-wire cable excited by a plane-wave electromagnetic field," *IEEE Trans. Electromagn. Compat.*, vol. EMC-22, no. 1, pp. 16-19, Feb. 1980.

[9]   B. Cannas, A. Fanni, and F. Maradei, "A neural network approach to predict the crosstalk in non-uniform multiconductor transmission lines," *In Proc. IEEE Int. Symp. Circuits Syst.*, Phoenix-Scottsdale, AZ, USA, pp. 573-576, June 2002.

[10]   F. Dai, G. Bao, and D. Su, "Crosstalk prediction in non-uniform cable bundles based on neural network," *Proceedings of the 9th in Symp. on Antennas*, Propagation and EM Theory, Guangzhou, China, pp. 1043-1046, Nov. 2010.

[11]   C. Jullien, P. Besnier, M. Dunand, and I. Junqua, "Advanced modeling of crosstalk between an unshielded twisted pair cable and an unshielded wire above a ground plane," *IEEE Trans. Electromagn. Compat.*, vol. 55, no. 1, pp. 183-194, Feb. 2013.

[12]   A. Shoory, M. Rubinstein, A. Rubinstein, and F. Rachidi, "Simulated NEXT and FEXT in twisted wire pair bundles," *Proc. EMC Eur. Symp.*, York, U.K., pp. 266-271, Sept. 2011.

[13] M. Tang and J. Mao, "A precise time-step integration method for transient analysis of lossy nonuniform transmission lines," *IEEE Trans. Electromagn Compat.*, vol. 50, no. 1, pp. 166-174, Feb. 2018.

[14] C. P. Yang, W. Yan, Y. Zhao, Y. Chen, C. M. Zhu, and Z. B. Zhu, "Analysis on RLCG parameter matrix extraction for multi-core twisted cable based on back propagation neural network algorithm," *IEEE Access*, vol. 7, pp. 126315-126322, Aug. 2019.

[15] C. Huang, Y. Zhao, W. Yan, Q. Liu, and J. Zhou, "A new method for predicting crosstalk of random cable bundle based on BAS-BP neural network algorithm," *IEEE Access*, vol. 8, pp. 20224-20232, Jan. 2020.

[16] Q. Liu, Y. Zhao, W. Yan, C. Huang, A. Mueed, and Z. Meng, "A novel crosstalk estimation method for twist non-uniformity in twisted-wire pairs," *IEEE Access*, vol. 8, pp. 38318-38326, Feb. 2020.

[17] X. Yi, "Selection of initial weights and thresholds based on the genetic algorithm with the optimized back-propagation neural network," *In Proc. 12th Int. Conf. Fuzzy Syst. Knowl. Discovery (FSKD)*, Zhangjiajie, China, pp. 173-177, Aug. 2015.

[18] T. Rashid, *Make Your Own Neural Network*. 1st ed., Charleston, SC, USA: CreateSpace Independent Publishing Platform, 2016.

[19] M. Hassoun, *Fundamentals of Artfificial Neural Networks. Cambridge*, MA, USA: Bradford Book, 2003.

[20] H. Khan, X. Cao, S. Li, V. N. Katsikis, and L. Liao, "BAS-ADAM: an ADAM based approach to improve the performance of beetle antennae search optimizer," *IEEE/CAA Journal of Automatica Sinica*, vol. 7, no. 2, pp. 461-471, Mar. 2020.

[21] W. Bo, W. Jindong, Z. Hengwei, and Y. Dingkun, "Dynamic service selection based on chaotic mutation multi-objective particle swarm algorithm," *Proceedings of 2013 3rd International Conference on Computer Science and Network Technology*, Dalian, pp. 113-117, Oct. 2013.

[22] CST Microwave Studio, ver. 2008, Computer Simulation Technology, Framingham, MA, 2008.

Yanxing Ji was born in Jiangsu Province, China. He received the B.S degree in school of Yancheng Institute of Technology, Yancheng, China, in 2018. He is currently working toward the Master's degree in Electrical Engineering at Nanjing Normal University, Nanjing, China. His main research interests include multi-conductor transmission lines and EMC.

Wei Yan Doctor & Assoc. Professor from Nanjing Normal University. He obtained the Physics and Electronics Ph.D. and Electrical Engineering M.S. from Nanjing Normal University in 2014 and 2011. He is the Senior Member of China Electrical Technology Association and the evaluation expert of the Electromagnetic Compatibility Calibration Specification of China.

Yang Zhao received his B.E., M.E., and Ph.D. degree all in Power Electronic Technology from Nanjing University of Aeronautics and Astronautics, Nanjing, China, in 1989 and 1992, and 1995, respectively. He is currently the Professor with Nanjing Normal University. His research interests are in the areas of Electromagnetic Compatibility, Power Electronics and Automotive Electronics.

Chao Huang was born in Anhui Province, China. He received the B.S degree in school of Electrical Engineering and Automation from Anhui University of Technology, Maanshan, China, in 2018. He is currently working toward the Master's degree in Electrical Engineering at Nanjing Normal University, Nanjing, China. His main research interests include multi-conductor transmission lines and EMC.

Shiji Li received his Electrical Engineering M.S. from Nanjing Normal University in 2013. He is currently the Lecturer with Nanjing Normal University. His research interests are in the areas of Electromagnetic Compatibility and Industrial electric Automation.

Jianming Zhou was born in Jiangsu Province, China. He received the B.S degree in school of Electrical Engineering and Automation from Tianping College of Suzhou University of Science and Technology, Suzhou, China, in 2019. He is currently working toward the Master's degree in Electrical Engineering at Nanjing Normal University, Nanjing, China. His major research interests include new technology of electrical engineering.